

Direct Observation of Charge Order in an Epitaxial NdNiO₃ Film

U. Staub,¹ G. I. Meijer,² F. Fauth,^{1,3} R. Allenspach,² J. G. Bednorz,² J. Karpinski,⁴ S. M. Kazakov,⁴
L. Paolasini,³ and F. d'Acapito³

¹Swiss Light Source, Paul Scherrer Institute, CH-5232 Villigen PSI, Switzerland

²IBM Research, Zurich Research Laboratory, CH-8803 Rüschlikon, Switzerland

³European Synchrotron Research Facility, BP 220, F-38043 Grenoble Cedex, France

⁴Laboratorium für Festkörperphysik, ETH-Zürich, CH-8093 Zurich, Switzerland

(Received 6 September 2001; published 8 March 2002)

The first direct observation of charge order of Ni^{3+ δ'} and Ni^{3- δ} by resonant x-ray scattering experiments in an epitaxial film of NdNiO₃ is reported. A quantitative value of $\delta + \delta' = (0.45 \pm 0.04)e$ was obtained. The temperature dependence of the charge order deviates significantly from those of the magnetic moment and crystallographic structure. This might be an indication of a difference in their fluctuation time scales. These observations are discussed in terms of the temperature-driven metal-insulator transition in the RNiO₃ family.

DOI: 10.1103/PhysRevLett.88.126402

PACS numbers: 71.30.+h, 71.45.Lr, 75.40.Cx, 78.70.Ck

The 3d transition-metal oxides exhibit a fascinating variety of physical properties ranging from high- T_c superconductivity to colossal magnetoresistance. One of the long-standing issues associated with these strongly correlated electron systems is the microscopic origin of the metal-to-insulator transitions and the nature of their ground state.

A prototype bandwidth-controlled metal-insulator transition is RNiO₃, R being the trivalent rare-earth ions (La to Lu) or Y [1]. RNiO₃ crystallizes in the orthorhombically distorted perovskite structure $Pbnm$ with unit cell $\sqrt{2}a_p \times \sqrt{2}a_p \times 2a_p$, where a_p is the perovskite cell parameter. The nominal valence of Ni is 3+ with d -electron configuration $t_{2g}^6 e_g^1$ and spin $S = 1/2$. RNiO₃ has a small charge-transfer energy and can be regarded as a self-doped Mott insulator [2]. In the RNiO₃ series, LaNiO₃ has the largest one-electron bandwidth and is metallic down to the lowest temperatures. All other RNiO₃ compounds have an insulating ground state; i.e., they have a charge-transfer gap between the O-2p and the Ni-3d upper Hubbard band. RNiO₃ exhibits a thermally driven metal-insulator transition at T_{MI} and a further transition to long-range antiferromagnetic order at $T_N \leq T_{MI}$. Examples are NdNiO₃ with $T_{MI} = T_N = 200$ K, SmNiO₃ with $T_{MI} = 400$ K and $T_N = 225$ K [3], and YNiO₃ with $T_{MI} = 480$ K and $T_N = 205$ K [4]. Associated with T_{MI} is a slight but abrupt expansion of the crystallographic unit cell, which causes a narrowing of the bandwidth, eventually leading to the opening of a gap at the Fermi surface [3,5].

Below T_N , RNiO₃ shows an unusual magnetic ordering with propagation vector $(1/2, 0, 1/2)$, with respect to the orthorhombic unit cell [5–7]. This corresponds to an up-up-down-down stacking of ferromagnetic planes along the pseudocubic [111] direction. As the twofold degenerate orbital e_g is singly occupied, one may expect a significant Jahn-Teller distortion and associated orbital ordering (of $x^2 - y^2/3z^2 - r^2$ type) in the insulating state of the

RNiO₃ compounds [6]. Such a formation of an orbital superlattice could indeed explain the unusual magnetic ordering. In addition, the observed large isotope effect on T_{MI} [8] is an indication of a strong interaction with the lattice, and points to the presence of Jahn-Teller polarons [9]. However, thus far, no evidence for a Jahn-Teller distortion has been found. Moreover, it was argued that the orbital ordered state has a relatively high energy, suggesting that it is not responsible for the magnetic structure [10,11].

Recently, indirect evidence was found from high-resolution synchrotron powder diffraction that the strongly distorted members of the RNiO₃ series, for example YNiO₃, have a charge-ordered ground state (also called charge disproportionation) [4,12,13]. This interpretation is based on the observed symmetry lowering to monoclinic $P2_1/n$ crystal structure ($\beta = 90.08^\circ$) at $T < T_{MI}$, which breaks up the single Ni site in the metallic phase into two individual crystallographic sites when the charge-transfer gap opens ($Pbnm$ at $T > T_{MI}$ to $P2_1/n$ at $T < T_{MI}$). Thus far, no indication of a monoclinic distortion as in YNiO₃ has been found [12] for the larger rare-earth atoms Pr, Nd, Sm, and Eu, based on high-resolution diffraction. Indications for symmetry breaking were recently reported in an electron diffraction and Raman study on NdNiO₃ [14], supporting the idea that charge order may occur for all R ions.

In this Letter, we present resonant x-ray scattering data on an epitaxial film of NdNiO₃. This technique is ideal to study charge and orbital ordering [15] because the structure factor strongly depends on the electronic structure in the vicinity of an absorption edge of an ion. The observed site-selective electronic information is put into the context of the discussion of magnetic order and the metal-insulator transition. Thus far, the lack of single crystals has precluded such experiments on the nickelate series.

High-quality epitaxial films of NdNiO₃ have been grown on (001)-oriented NdGaO₃ substrates ($Pbnm$) by pulsed laser deposition. The lattice constants of the film grown

along the c axis are in plane expanded $a \approx b = 5.48 \text{ \AA}$ and $c = 7.59 \text{ \AA}$ compared to polycrystalline NdNiO_3 ($a = 5.38 \text{ \AA}$, $b = 5.39 \text{ \AA}$, $c = 7.61 \text{ \AA}$). As a target, we used polycrystalline NdNiO_3 synthesized as in Ref. [16]. The films are deposited in 0.3 mbar oxygen atmosphere at $T = 740 \text{ }^\circ\text{C}$. After deposition, the sample is cooled slowly in $\text{PO}_2 = 1$ bar. The energy of the KrF excimer laser was 800 mJ at 5 Hz. The resistivity of the film was measured with the conventional four-probe technique. No impurity phases have been detected with Cu K_α radiation. The rocking curve full width at half maximum of the film is 0.14° (inset of Fig. 1). Synchrotron x-ray scattering experiments have been performed at ID20 of the ESRF. A Cu (222) crystal was used for polarization analysis. The energy resolution was approximately 1 eV. The x-ray absorption data were collected at Gilda CRG (BM08) of the ESRF in fluorescence mode at ambient temperature.

Figure 1 shows the resistivity of the 500- \AA -thick NdNiO_3 film. A first-order metal-insulator transition is observed at approximately 170 and 150 K on the heating and cooling runs, respectively. T_{MI} is lower than in polycrystalline NdNiO_3 , probably because of epitaxial strain. The resonant x-ray scattering experiments focused on reflections of type $(0hl)$ and $(h0l)$, with h and l odd. In $Pbnm$ symmetry, these reflections have no contribution from the Ni site. Figure 2 shows the energy dependence of the (105) and (015) reflections with σ - σ polarization in the insulating state at 20 K. The spectrum of the (105) shows a strong maximum [minimum for (015)] at 8344 eV, approximately 10 eV above the Ni K -edge (8333 eV). This shows that these reflections contain a significant contribution from the electronic states of the Ni ions. Therefore, the resonant x-ray scattering data clearly indicate that, for $T < T_{\text{MI}}$, the $Pbnm$ symmetry is lowered ($P2_1/n$). This symmetry breaking has not been observed with high-resolution powder diffraction for NdNiO_3 [12]. No indication of orbital order was found from the measurements with σ - π polarization. Figure 3 shows the resonant scattering of the (105) reflection for different temperatures. The nonresonant x-ray intensities as well as the energy dependence decrease for increasing

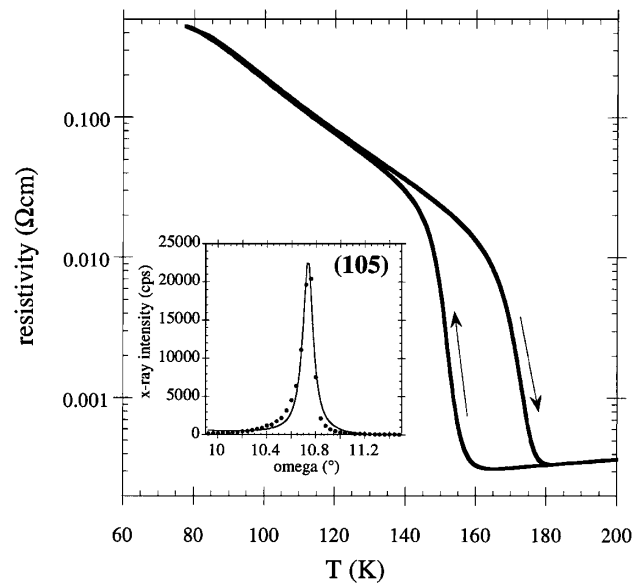


FIG. 1. The resistivity of epitaxial films of NdNiO_3 on NdGaO_3 . Inset: Rocking curve of the (105) reflection taken at 190 K.

temperatures. Above T_{MI} , the scattering is independent of the energy, and there no longer is a resonant contribution from Ni. This confirms that there is a single electronic configuration of the Ni ions in the metallic phase ($T > T_{\text{MI}}$).

The energy dependence of the x-ray intensity is $I \propto |F(\mathbf{Q}, E)F^*(\mathbf{Q}, E)|$. $F(\mathbf{Q}, E)$ is the structure factor given by $F(\mathbf{Q}, E) = \sum_i f_i(\mathbf{Q}, E)e^{i\mathbf{Q}\cdot\mathbf{R}_i} \delta(\mathbf{Q} - \boldsymbol{\tau})$, neglecting the Debye-Waller term. Here, \mathbf{Q} and E are the x-ray momentum transfer and the x-ray energy, $f_i(\mathbf{Q}, E)$ is the x-ray scattering factor of the i th ion at position \mathbf{R}_i within the unit cell, and $\boldsymbol{\tau}$ is a reciprocal lattice vector. $f_i(\mathbf{Q}, E)$ is given by $f_i(\mathbf{Q}, E) = f_i^0(\mathbf{Q}) + f_i'(E) + if_i''(E)$, where $f_i^0(\mathbf{Q})$ corresponds to the Thompson scattering and $f_i'(E)$ and $if_i''(E)$ to the real and imaginary energy-dispersive correction factors, respectively. In monoclinic symmetry $P2_1/n$, there are two inequivalent Ni sites labeled Ni_I and Ni_{II} . The structure factor $F(\mathbf{Q}, E)$ of the (015) and (105) reflections is then given by

$$\begin{aligned} F_{015}(\mathbf{Q}, E) &= A_{\text{O,Nd}}(\mathbf{Q}) + 2\Delta f_{\text{Ni}}^0(\mathbf{Q}) + 2\Delta f_{\text{Ni}}'(E) + 2i\Delta f_{\text{Ni}}''(E), \\ F_{105}(\mathbf{Q}, E) &= B_{\text{O,Nd}}(\mathbf{Q}) - 2\Delta f_{\text{Ni}}^0(\mathbf{Q}) - 2\Delta f_{\text{Ni}}'(E) - 2i\Delta f_{\text{Ni}}''(E), \end{aligned} \quad (1)$$

where $\Delta f_{\text{Ni}}'(E) = f_{\text{Ni}_I}'(E) - f_{\text{Ni}_{II}}'(E)$, $\Delta f_{\text{Ni}}''(E) = f_{\text{Ni}_I}''(E) - f_{\text{Ni}_{II}}''(E)$, $\Delta f_{\text{Ni}}^0 = f_{\text{Ni}_I}^0 - f_{\text{Ni}_{II}}^0$, and $A_{\text{O,Nd}}$ and $B_{\text{O,Nd}}$ correspond to the O and Nd contributions to the structure factor. For a single electronic Ni configuration $f_{\text{Ni}_I} = f_{\text{Ni}_{II}}$, $F_{015} = A_{\text{O,Nd}} = 0$, and $F_{105} = B_{\text{O,Nd}}$. An energy dependence of the Bragg reflections occurs only when $f_{\text{Ni}_I} \neq f_{\text{Ni}_{II}}$. Therefore, our data directly prove that NdNiO_3 has a long-range charge-ordered ground state with the two distinct Ni sites, $\text{Ni}^{3+\delta'}$ and $\text{Ni}^{3-\delta}$.

To determine the size of this charge order and the site-selective electronic structure of the Ni ions, we will now discuss the Ni K -edge energy shift between Ni_I and Ni_{II} . The resonant x-ray scattering intensities for the (105) reflections [Eq. (1)] can be approximated by $I(E)_{(105)} \propto (B'_{\text{O,Nd}})^2 - 4B'_{\text{O,Nd}}\Delta f_{\text{Ni}}'(E)$ (using $B''_{\text{O,Nd}} \gg B''_{\text{O,Nd}}^{(105)}$, with ' and '' indicating the real and imaginary part). This shows that the resonant scattering intensity depends linearly on the difference of the real part

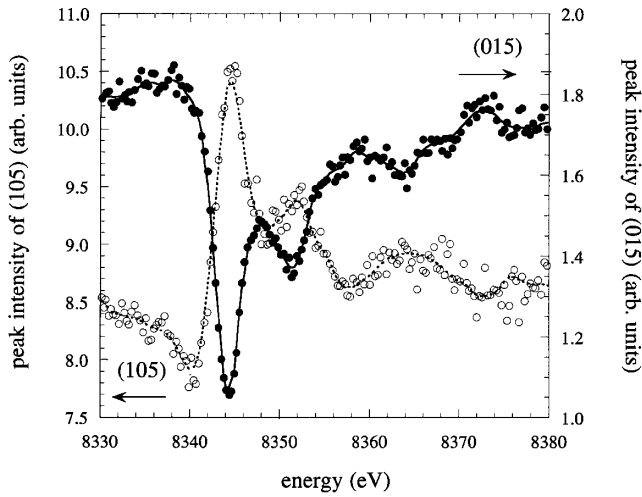


FIG. 2. Energy-dependent x-ray intensity of the (015) and (105) reflections taken at 20 K with σ - σ polarization. The lines are guides to the eye.

of the scattering factors $f'_{\text{Ni}_I}(E) - f'_{\text{Ni}_{II}}(E)$. On the other hand, the x-ray absorption spectrum is sensitive to the sum $f''_{\text{Ni}_I}(E) + f''_{\text{Ni}_{II}}(E)$. From the *sum* and *difference*, and the Kramers-Kronig relation, the site-selective real and imaginary parts of the scattering factors of the Ni_I and Ni_{II} sites are obtained (Fig. 4). The energy shift between the Ni_I and Ni_{II} -site scattering factors at the Ni K -edge is found to be 0.90 ± 0.08 eV. The Ni K -edge shift for different electronic states of Ni has been studied for LaNiO_{3-x} , La_2NiO_4 , and LaNiO_2 [17]. A linear dependence of the Ni valence as a function of K -edge shift for these oxides was found. Using these results, the 0.9-eV

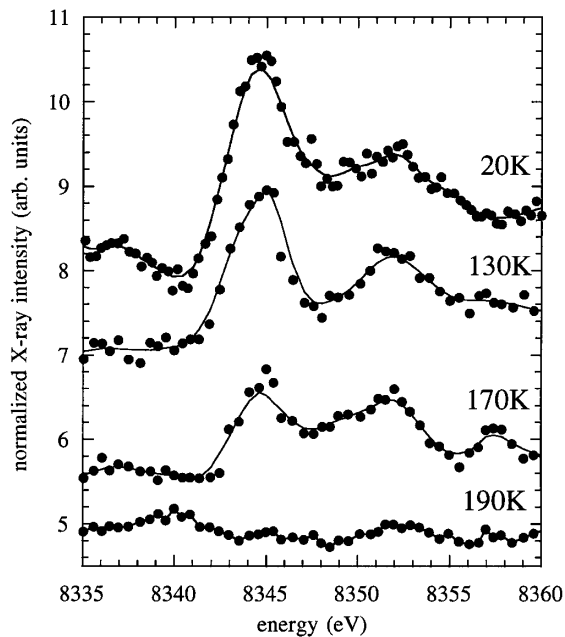


FIG. 3. Energy-dependent x-ray intensity of the (105) reflection for selected temperatures. The lines are guides to the eye.

K -edge shift translates into $\delta + \delta' = 0.42 \pm 0.04e$ in the ground state. Alternatively, the 0.9-eV shift can be compared with the energy shift of 2 eV between the $3d^7$ and $3d^8\bar{L}$ (\bar{L} denotes a ligand hole) configurations as obtained by multiple scattering calculations [18], which results in a similar value of $\delta + \delta' = 0.45 \pm 0.04e$. These values are smaller than those obtained by bond-valence sum calculations for the monoclinic distorted RNiO_3 with smaller R ions [13] of $\delta \approx \delta' \approx 0.3e$ or $\delta + \delta' \approx 0.6e$.

X-ray absorption spectroscopy and Hartree-Fock calculations [19] found that the Ni average electronic state is not $3+$. They propose a mixture of approximately 70% $3d^7$ and 30% $3d^8\bar{L}$, corresponding to a Ni average valence of 2.7 and implying that $\delta' \neq \delta$. Taking this into account, we find that the Ni_I and Ni_{II} sites have valences of approximately $3+$ and $2.5+$, respectively ($\delta' \approx 0$ and $\delta \approx 0.5e$). As $3d^7$ and $3d^8\bar{L}$ correspond to $\text{Ni}^{3+} - \text{O}^{2-}$ and $\text{Ni}^{2+} - \text{O}^-$ configurations, respectively, this result indicates charge order on Ni as well as O sites. This is in contrast to the prediction of the Hartree-Fock calculations [2] that yielded charge order on Ni for the smaller R ions (e.g., Ho, Y) and on O for the larger R ions (e.g., Nd).

The charge-order order parameter can be extracted from the temperature dependence of the integrated x-ray intensity of the (105) reflection. Because $B_{\text{O,Nd}}^{(105)} \gg B_{\text{O,Ni}}^{(105)}$, the charge-order order parameter is, in good approximation, proportional to $\sqrt{I(E_{\text{res}})} - \sqrt{I(E_{\text{offres}})}$, where

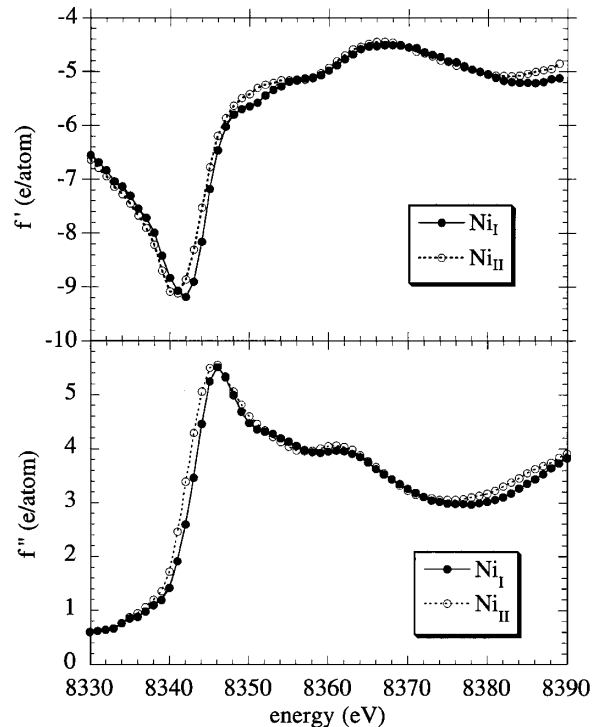


FIG. 4. Site-selective real (upper panel) and imaginary (lower panel) parts of the energy-dependent correction to the scattering factors of Ni.

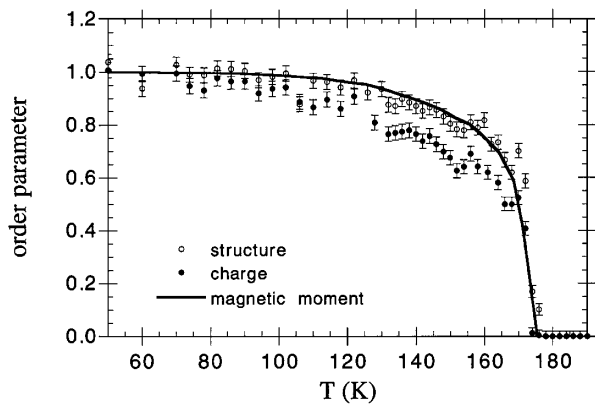


FIG. 5. The temperature dependence (heating) of the charge-order order parameter, structural order parameter, and magnetic moment (rescaled from Ref. [21]).

$E_{\text{res}} = 8344.5$ eV and $E_{\text{offres}} = 8330$ eV. The temperature dependence of the change in intensity off resonance is dominated by $(B_{\text{O,Nd}}^{(105)})^2$, i.e., the square of the “crystallographic” structural order parameter. Note that the direct contribution of the charge order to the structure factor off resonance is negligible [the difference in the Thomson scattering being $<0.13e$ [20] at the (105) and (015) reflections]. Figure 5 shows the temperature dependence (on heating) of the charge-order order parameter and the structural order parameter extracted from the integrated intensities of the (105) reflection. These curves are compared with the ordered magnetic moment of the Ni ions in polycrystalline NdNiO₃ taken from neutron scattering [21] (rescaled to unity and with the same T_N for the magnetic moment). The structural and magnetic order parameters are identical within experimental accuracy. The charge-order order parameter, however, behaves differently. This may indicate a difference in the fluctuation time scales of the magnetic moment and structure as compared to the charge. NdNiO₃ is highly conducting; i.e., the charge fluctuations above T_{MI} are very fast and inhibit magnetic order. This is in contrast to, for example, the RBaCo₂O₅-type cobaltites, for which $T_N > T_{\text{MI}}$ ($T_N \approx 340$ K and $T_{\text{MI}} \approx 210$ K [22]). For these cobaltites, the conductivity is smaller than in RNiO₃ [22] at $T > T_{\text{MI}}$. This means that the charge fluctuations are much slower, and magnetic order can occur already at temperatures above T_{MI} . If NdNiO₃ had a comparably low conductivity, one would expect the magnetic order to occur at a higher temperature [23]. In NdNiO₃, the magnetic moments can already saturate while the charge fluctuations are slowing down. The structure, for which the fluctuations are slow (massive particles involved), can relax only when the charge fluctuations are slow enough, which could explain their different observed order parameters. These results were obtained on a strained epitaxial

film, and care has to be taken when compared with bulk properties (e.g., magnetic order parameter).

In conclusion, we directly observe charge order ($\text{Ni}^{3+\delta'}$ and $\text{Ni}^{3-\delta}$) at the metal-insulator transition in NdNiO₃, using resonant x-ray scattering. This finding shows that the metal-insulator transition in NdNiO₃ can be understood on the basis of charge order. This charge order can also account for the unusual magnetic propagation vector, rendering models with orbital order obsolete. The size of the charge order was determined to be $\delta + \delta' = 0.45 \pm 0.04e$. The site-selective electronic states of Ni_I and Ni_{II} are determined to be approximately $3d^7$ and a 50% mixture of $3d^7$ and $3d^8L$, respectively. Finally, the order parameters of the magnetic moment and the structural deviation differ significantly from the charge-order parameter, providing insight into the differences of the time scales in the fluctuations.

We thank C. Rossel and M. Medarde for fruitful discussion, D. Gruetzmacher for the Cu K_α x-ray characterization of the film and O. Zaharko (both at the PSI) for the inverse Kramers-Kronig transform code.

-
- [1] M. Imada, A. Fujimori, and Y. Tokura, *Rev. Mod. Phys.* **70**, 1039 (1998).
 - [2] T. Mizokawa, D. I. Khomskii, and G. A. Sawatzky, *Phys. Rev. B* **61**, 11 263 (2000).
 - [3] J. B. Torrance *et al.*, *Phys. Rev. B* **45**, R8209 (1992).
 - [4] J. A. Alonso *et al.*, *Phys. Rev. Lett.* **82**, 3871 (1999).
 - [5] J. L. García-Muñoz *et al.*, *Phys. Rev. B* **46**, 4414 (1992).
 - [6] J. Rodríguez-Carvajal *et al.*, *Phys. Rev. B* **57**, 456 (1998).
 - [7] M. L. Medarde, *J. Phys. Condens. Matter* **9**, 1679 (1997).
 - [8] M. Medarde *et al.*, *Phys. Rev. Lett.* **80**, 2397 (1998).
 - [9] G.-m. Zhao *et al.*, *Nature (London)* **381**, 676 (1996).
 - [10] T. Mizokawa and A. Fujimori, *Phys. Rev. B* **54**, 5368 (1996).
 - [11] T. Mizokawa and A. Fujimori, *Phys. Rev. B* **51**, R12 880 (1995).
 - [12] J. A. Alonso *et al.*, *J. Am. Chem. Soc.* **121**, 4754 (1999).
 - [13] J. Alonso *et al.*, *Phys. Rev. B* **61**, 1756 (2000).
 - [14] M. Zaghrioui *et al.*, *Phys. Rev. B* **64**, 081102(R) (2001).
 - [15] Y. Murakami *et al.*, *Phys. Rev. Lett.* **80**, 1932 (1998).
 - [16] P. Lacorre *et al.*, *J. Solid State Chem.* **91**, 225 (1991).
 - [17] M. Crespín, P. Levitz, and L. Gatineau, *J. Chem. Soc. Faraday Trans.* **79**, 1181 (1983).
 - [18] J. García *et al.*, *Phys. Rev. B* **52**, 15 823 (1995).
 - [19] M. Medarde *et al.*, *Phys. Rev. B* **46**, 14 975 (1992).
 - [20] E. N. Maslen, A. G. Fox, and M. A. O’Keefe, *International Tables for Crystallography*, edited by A. J. C. Wilson and E. Prince (Kluwer, Dordrecht, 1992), p. 548.
 - [21] J. L. García-Muñoz, J. Rodríguez-Carvajal, and P. Lacorre, *Europhys. Lett.* **20**, 241 (1992).
 - [22] E. Suard *et al.*, *Phys. Rev. B* **61**, R11871 (2000).
 - [23] I. Vobornik *et al.*, *Phys. Rev. B* **60**, R8426 (1999).